

ARTICLES

Optimal reconstruction of the input signal in resonant gravitational wave detectors: Data processing algorithm and physical limitations

A. Ortolan and G. Vedovato

INFN, Laboratori Nazionali di Legnaro, Via Romea 4, I-35020 Legnaro, Padova, Italy

M. Cerdonio and S. Vitale

Dipartimento di Fisica, Università di Trento, and INFN Gruppo di Trento, Sez. Di Padova, I-38050 Povo, Trento, Italy

(Received 14 January 1994)

We discuss a method of data filtering for a resonant gravitational wave detector that allows an optimal reconstruction of the input signal. The method consists of the estimate, by optimal Wiener filtering, of the amplitude of the Karhunen-Loève components of the signal at the antenna input, and only needs the assumption that the signal has a finite duration. After discussing an application of the method to a simplified model for a resonant antenna, we present a practical application to the reduction of the data from a room temperature antenna.

PACS number(s): 04.80.Nn, 95.55.Ym, 95.75.Pq

INTRODUCTION

There have been many studies over the years [1] aimed at assessing the time shape and relevant parameters of the gravitational radiation bursts emitted during different collapse scenarios. These studies show that the main burst features, such as the spectral content, the center frequency, the duration, etc., depend on the details of the collapse. On the other hand, the available observational knowledge has not allowed one, up to now, to predict with enough confidence which one of the proposed scenarios, if any, is the most probable candidate for a detectable emission of gravitational waves. The consequence of all this is that, despite the fact that any optimal detection method needs some assumption about the expected signal, any cautious detection strategy should keep the number of those assumptions to the smallest possible amount.

Resonant gravitational wave detectors have comparatively narrow bandwidths. The ultracryogenic ones currently under development promise to have post-detection bandwidths in the range 20–50 Hz, with resonant frequencies of the order of 1 kHz. The signal-to-noise ratio per unit frequency consists of a few close narrow minima merging in the wideband noise of the amplifier [2]. With this kind of effective post-detection band, it is not immediate to assess what the independent parameters are that can be extracted from the signal and what the related data reduction methods are to extract them from the raw data.

In this paper we describe an optimal method of signal detection that, first needs only to assume that the signal has some finite duration, a very reasonable approximation for gravitational bursts, and, second, gives in a very natural way the statistically independent param-

eters that can be extracted from the signal. The method consists of the standard estimate [3], by optimal Wiener filtering, of the amplitude of the Karhunen-Loève components of the signal *at the antenna input*. After discussing an application of the method to a simplified model for a resonant antenna, we shortly present, as an example, a practical application to the reduction of the data from a room temperature antenna.

PRINCIPLE OF THE METHOD

We will assume that a gravitational wave detector can be described as a linear, time-invariant device whose input is the metric perturbation $h(t)$ and whose output is some electrical signal $V(t)$ buried in additive Gaussian noise. With this assumption,

$$V(t) = n(t) + \int_0^\infty H(t')h(t-t')dt', \quad (1)$$

where $n(t)$ is the total output noise, with spectral density $S(\omega)$, and $H(t)$ is the impulse response of the detector.

We will also assume that the signal $h(t)$ has a finite duration T :

$$h(t) = 0 \text{ if } |t| \geq \frac{T}{2}. \quad (2)$$

A standard technique, known as the Karhunen Loève expansion [3], used to extract the available information from a signal of duration T buried in the noise, is to assume that the signal can be expanded in a series of some set of orthonormal functions $\phi_k(t)$,

$$h(t) = \sum_{k=0}^{\infty} c_k \phi_k(t) \quad (3)$$

and to choose the ϕ_k 's such that the minimum-variance linear estimates of the c_k 's are statistically independent. With the expansion in Eq. (3), the antenna output is given by

$$V(t) = n(t) + \sum_{k=0}^{\infty} c_k \int_0^{\infty} H(t') \phi_k(t-t') dt'. \quad (4)$$

According to the Wiener optimal filter theory, the minimum-variance zero-bias linear estimate of c_k , obtained from the output data $V(t)$, is

$$\hat{c}_k = \int_{-\infty}^{\infty} C_k(-t) V(t) dt, \quad (5)$$

with $C_k(t)$ a function whose Fourier transform is

$$C_k(\omega) = \sum_{j=1}^N \sigma_{kj} \frac{H^*(\omega) \phi_j(\omega)}{S(\omega)}, \quad (6)$$

where $\phi_j(\omega)$ and $H(\omega)$ are the Fourier transforms of $\phi_j(t)$ and $H(t)$, respectively.

The inverse of the matrix σ_{kj} , $(\sigma^{-1})_{kj}$, is given by

$$(\sigma^{-1})_{kj} = \left[\frac{1}{2\pi} \int_{-\infty}^{\infty} \frac{|H(\omega)|^2}{S(\omega)} \phi_k(\omega) \phi_j^*(\omega) d\omega \right], \quad (7)$$

and it can be demonstrated that

$$\langle \hat{c}_k \hat{c}_j \rangle - \langle \hat{c}_k \rangle \langle \hat{c}_j \rangle = \sigma_{kj}, \quad (8)$$

where the angular brackets indicate the statistical average.

In order for the estimates \hat{c}_k to be statistically independent, as in the Karhunen-Loève expansion, one needs

$$\begin{aligned} & \frac{1}{2\pi} \int_{-\infty}^{\infty} \frac{|H(\omega)|^2}{S(\omega)} \phi_k(\omega) \phi_j^*(\omega) d\omega \\ &= \frac{1}{\sigma_{\delta}^2} \int_{-T/2}^{T/2} dt \phi_j(t) \int_{-T/2}^{T/2} G(t-t') \phi_k(t') dt' = \frac{\lambda_j}{\sigma_{\delta}^2} \delta_{kj}, \end{aligned} \quad (9)$$

with λ_j some positive constant and δ_{kj} the Kroenecker delta. The function $G(t)$ in Eq. (9) is defined as the Fourier transform of

$$G(\omega) = \frac{|H(\omega)|^2 / S(\omega)}{(1/2\pi) \int_{-\infty}^{\infty} [|H(\omega)|^2 / S(\omega)] d\omega} \quad (10)$$

and

$$\sigma_{\delta}^2 = \frac{1}{(1/2\pi) \int_{-\infty}^{\infty} [|H(\omega)|^2 / S(\omega)] d\omega}. \quad (11)$$

σ_{δ}^2 is, according to Wiener-Kolmogorov theory, the min-

imum variance of the estimate of the amplitude A of a δ -like signal $h(t) = A\delta(t)$.

It is straightforward to check that Eq. (9) is satisfied if

$$\int_{-T/2}^{T/2} G(t-t') \phi_j(t') dt' = \lambda_j \phi_j(t) \quad (12)$$

and

$$\int_{-T/2}^{T/2} \phi_k(t) \phi_j(t) dt = \delta_{kj}, \quad (13)$$

i.e., if the functions $\phi_k(t)$ are the orthonormal eigenfunctions of the integral equation (12) and if the λ_j 's are its eigenvalues.

From Eqs. (7)-(9), (12), and (13), one gets

$$\sigma_{kj} = \sigma_{\delta}^2 \frac{\delta_{kj}}{\lambda_j}, \quad (14)$$

and the filter function $C_k(t)$ has the Fourier transform

$$C_k(\omega) = \frac{\sigma_{\delta}^2 H^*(\omega) \phi_k^*(\omega)}{\lambda_k S(\omega)} = \frac{\phi_k^*(\omega)}{\lambda_k} C_{\delta}(\omega). \quad (15)$$

Here $C_{\delta}(\omega) = \sigma_{\delta}^2 H^*(\omega) / S(\omega)$ is the optimum filter function one should apply to the output data in order to estimate the amplitude of a δ signal at the input.

Equation (15) shows that the estimate can be done, as usual with Wiener filters, in two stages: first, by filtering the data with the filter $C_{\delta}(\omega)$ to obtain the function $V'(t)$,

$$V'(t) = \int_{-T/2}^{T/2} C_{\delta}(t-t') V(t') dt', \quad (16)$$

and, second, by calculating the amplitudes of the expansion of $V'(t)$ in the $\phi_k(t)$'s according to

$$\hat{c}_k = \frac{1}{\lambda_k} \int_{-T/2}^{T/2} \phi_k(t) V'(t) dt. \quad (17)$$

Equation (12) shows that the set of functions $\phi_k(t)$ is the Karhunen-Loève orthonormal set of the noise at the output of the filter $C_{\delta}(\omega)$, as this has a spectrum $\sigma_{\delta}^2 G(\omega)$. The method reduces then to filtering the data as if looking for a δ -function signal and then to expand the output of the filter into its independent Karhunen-Loève components.

At the end of this section we want to indicate a few properties of the above procedure we will use in the following.

Let us define the signal-to-noise ratio with which the k th component of a given signal $h(t) = Af(t)$ of "amplitude" A is measured:

$$R_k^2 = \frac{c_k^2}{\sigma_k^2} = \frac{\lambda_k c_k^2}{\sigma_{\delta}^2}, \quad (18)$$

with $c_k = \int_{-T/2}^{T/2} \phi_k(t) h(t) dt$.

It can easily be shown [3] that

$$\sum_{k=0}^{\infty} R_k^2 = \frac{A^2}{\sigma_A^2} = R_A^2. \quad (19)$$

Here σ_A^2 is the variance of the estimate of the amplitude A one would get from a Wiener filter matched to the signal $f(t)$, and thus R_A is the signal-to-noise ratio of this estimate. It follows that $R_k \leq R_A$.

A useful quantity we will use in the following is the total signal energy E_T at the output of the filter $C_\delta(\omega)$, defined as

$$E_T = \int_{-T/2}^{T/2} V'^2(t) dt, \quad (20)$$

a quantity which is measured with a signal-to-noise ratio R_E (see the Appendix):

$$R_E = \frac{\sum_{k=0}^{\infty} R_k^2 \lambda_k}{2 \left[\sum_{k=1}^{\infty} \lambda_k^2 \left(\frac{1}{2} + R_k^2 \lambda_k^2 \right) \right]^{1/2}}. \quad (21)$$

A second related quantity is the amplitude $|a| = \sqrt{E_T}$ whose signal-to-noise ratio is $R_{|a|} = 2R_E$.

AN EXAMPLE: THE GIFFARD MODEL FOR A RESONANT DETECTOR

Giffard [4] has proposed a useful simplified model for a resonant gravitational wave detector, where the antenna is represented by a simple harmonic oscillator of mass M , damping time τ , and angular frequency ω_0 , subject to a force $F(t) = L'M d^2h(t)/dt^2$. If the antenna is a long cylinder, as in practical experiments, the effective length L' is [5] $L' = (2/\pi^2)L$, with L the physical length of the antenna and M is one-half of its physical mass. The readout electronic chain is substituted in this model by a displacement transducer that converts the oscillator displacement to some output voltage signal. The transducer has two independent noise generators: One generates a white random force $F_n(t)$, with spectral density S_F , that adds up to the signal force $F(t)$ and that includes both the back action of the readout chain and the Brownian noise of the oscillator. The second generator is the source of a white displacement noise $x_n(t)$, with density S_x , and represents the noise added at the readout output. We write the spectral densities in terms of quanta as $S_F = KN \hbar/2$ and $S_x = N \hbar/2K$, with K a noise "impedance" with the physical dimensions of a spring constant.

With these assumptions and considering the force $F(t)$ as the input signal of the detector, one gets, for $G(t)$,

$$G(t) = e^{-|t|/2\tau_{\text{opt}}} \left[\cos(\omega_1 t) + \frac{1}{2\omega_1 \tau_{\text{opt}}} \sin(\omega_1 |t|) \right], \quad (22)$$

where

$$\omega_1^2 = \frac{\omega_0^2}{2} \left[\left(1 + \frac{K^2}{M^2 \omega_0^4} \right)^{1/2} + 1 \right] - \frac{1}{4\tau^2}$$

and

$$\frac{1}{\tau_{\text{opt}}^2} = \frac{1}{\tau^2} + 2\omega_0^2 \left[\left(1 + \frac{K^2}{M^2 \omega_0^4} \right)^{1/2} - 1 \right].$$

In practical detectors, $\omega_1 \approx \omega_0$ and $\tau_{\text{opt}} \approx M\omega_0/K \ll \tau$. $1/2\pi\tau_{\text{opt}}$ is usually called the post-detection bandwidth and, for the generation of detectors under development, is predicted [2] to be in the range 20–50 Hz.

The parameter σ_δ^2 is now

$$\sigma_\delta^2 = N \hbar \frac{M^2}{K} \frac{\omega_1^2}{\tau_{\text{opt}}^2} \approx N \hbar M \omega_0, \quad (23)$$

where in the last term of Eq. (23) we have assumed that $\tau_{\text{opt}} \ll \tau$.

Equation (12), with $G(t)$ given by Eq. (22), can be solved in closed form (see the Appendix). The solutions are of one of the two forms

$$\phi_k(t) = A_{k+} \cos(\omega_{k+} t) + A_{k-} \cos(\omega_{k-} t), \quad (24a)$$

$$\phi_k(t) = A_{k+} \sin(\omega_{k+} t) + A_{k-} \sin(\omega_{k-} t), \quad (24b)$$

with the (complex frequencies) ω_{k+} and ω_{k-} given by

$$\omega_{k\pm} = \omega_1 \left\{ \left(1 - \frac{1}{2q_{\text{opt}}^2} \right) \pm \left[\left(1 - \frac{1}{2q_{\text{opt}}^2} \right)^2 - \left(1 - \frac{2}{\lambda_k \omega_1 q_{\text{opt}}} \right) \right]^{1/2} \right\}^{1/2}, \quad (25)$$

where $q_{\text{opt}} = \omega_1 \tau_{\text{opt}}$. The eigenvalues λ_k are positive and bounded ($\sum_{k=1}^{\infty} \lambda_k = T$). They come in pairs of approximately the same value, corresponding to the functions in Eqs. (24a) and (24b), respectively. Here and in the rest, we will number them in decreasing order of magnitude.

For the largest eigenvalues, both ω_{k+} and ω_{k-} turn out to be real, and for realistic values of T and q_{opt} ($T\omega_1 \geq 2\pi$, $q_{\text{opt}} > 20$), both $1/2q_{\text{opt}}^2$ and $2/\lambda_k \omega_1 q_{\text{opt}}$ are small numbers. If this is the case,

$$\omega_{k\pm} \approx \omega_1 \pm \frac{\omega_1}{2q_{\text{opt}}} \left(\frac{2q_{\text{opt}}}{\lambda_k \omega_1} - 1 \right)^{1/2}.$$

Thus, as λ_k becomes smaller, both ω_{k-} and ω_{k+} tend to fall outside the optimal post-detection band $\omega_1 \pm \omega_1/2q_{\text{opt}}$ and the uncertainty on the corresponding c_k becomes larger.

In Fig. 1 we show the ratio T/λ_k for the first eigenvalues (in decreasing order of magnitude) as a function of $(\omega_+ - \omega_-)/2\omega_1$, for increasing values of T .

As expected from the discussion above, it can be calculated that, for large enough values of q_{opt} , the ratio λ_k/T depends only on the ratio $T\omega_1/q_{\text{opt}}$ so that Fig. 1 does not change very much by changing the value of q_{opt} , provided that one scales correspondingly the value of T .

Figure 1 shows that the eigenvalues quickly decrease with k . In addition, the spacing between neighboring eigenvalues decreases by increasing the duration T and so does the splitting between the corresponding values of $(\omega_{k+} - \omega_{k-})/2\omega_1$. Thus only if T is large enough, in comparison with τ_{opt} , is it then reasonable to expect

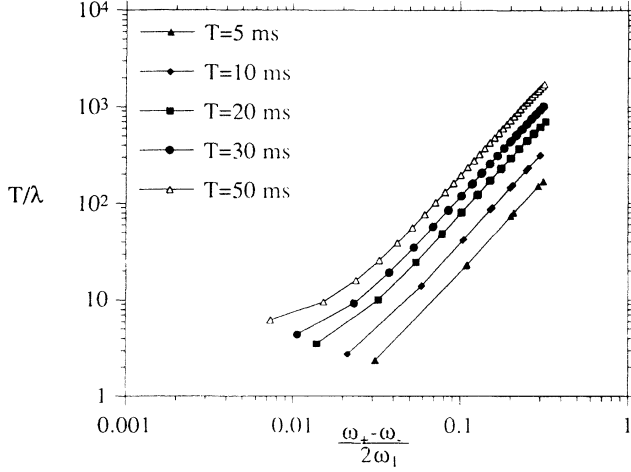


FIG. 1. Ratio T/λ as a function of $(\omega_+ - \omega_-)/2\omega_1$ for various values of T . $\omega_1 = 2\pi \times 1$ kHz and $q_{\text{opt}} = 30$.

that the signal components with $k > 1$ will have large signal-to-noise ratios.

To clarify this last point, we have calculated the amplitudes and signal-to-noise ratios for a specific signal which closely resembles many of the calculated expected gravitational signals:

$$h(t) = Ae^{-(t-t_0)^2/2\tau_p^2} \cos[\omega_p(t-t_0) + \phi], \quad (26)$$

with ω_p , τ_p , and t_0 the pulse center frequency, duration, and arrival time, respectively.

In Fig. 2 we show how both the $R_{k=1}$ and $R_{|a|}$ as a function of T for a short pulse arriving at the detector at time $t_0 = 0$. It can be seen that, for the $\tau_p = 0.5$ ms pulse considered, both c_1 (or c_2 for odd signals) and the “amplitude” $|a|$ have signal-to-noise ratios that never go below 60% of R_A , at least for T up to $T = 70$ ms. This

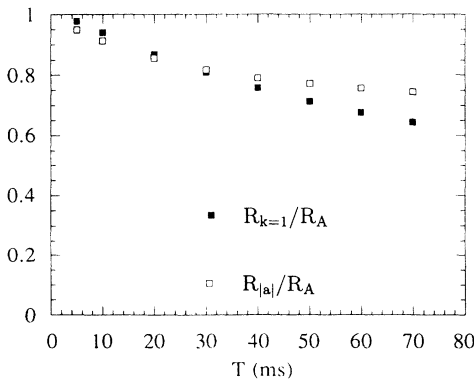


FIG. 2. Signal-to-noise ratio $R_{k=1}$ for the $k = 1$ component of the signal and that $R_{|a|}$ for the amplitude $|a|$, as a function of T . Both ratios are normalized to the signal-to-noise ratio R_A of a filter matched to the signal. To calculate $R_{|a|}$, $R_A = 4$. The signal is a pulse as in Eq. (30) with $\omega_p = \omega_1 = 2\pi \times 1$ kHz, $t_0 = 0$, and $\tau_p = 500 \mu\text{s}$. $q_{\text{opt}} = 30$.

shows that most of the information is carried by the $k = 1$ (or $k = 2$ for odd signals) component of the signal.

In addition, Fig. 2 shows that, when T becomes larger and larger and some information begins to be stored also in the $k > 2$ components, still $|a|$ is detected with a signal-to-noise ratio which is comparable to R_A and can then be used to monitor the data for the presence of the signal.

If τ_p becomes larger, both $R_{k=1}$ and $R_{|a|}$ increase toward R_A until τ_p is so large that the signal begins to be truncated and both ratios drop again (Fig. 3).

If the pulse has a phase $\phi \neq 0$, both the components in Eqs. (24a) and (24b) are excited. If a particular $\phi = \pi/2$, then the pulse is an odd function and the expansion includes only the terms in Eq. (24b).

More interesting is the situation if $t_0 \neq 0$. In this case the components with $k \neq 1, 2$ become more relevant, the energy is distributed over many components, and the signal-to-noise ratio on each one can drop significantly. The amplitude $|a|$, however, is still measured with a large signal-to-noise ratio (Fig. 4).

In summary, the main conclusion of this section is that the first few components of the expansion above, together with the amplitude $|a|$, can be measured with a signal-to-noise ratio comparable to that one would get from full knowledge of the incoming signal. Despite the fact that the above conclusion has been derived on the basis of a specific shape of the signal, it is likely that it is of general validity for all “pulse-shaped” signals, provided that the time length T has correctly been chosen to be longer than any incoming signal duration.

We note at the end that a practical application of the method of the process of real signals should first divide the time axis in intervals of duration T and should then apply the expansion to the data in each interval. Figure 4 suggests that two neighboring intervals should overlap by an interval of duration $T/2$ to avoid missing a large fraction of the signal energy.

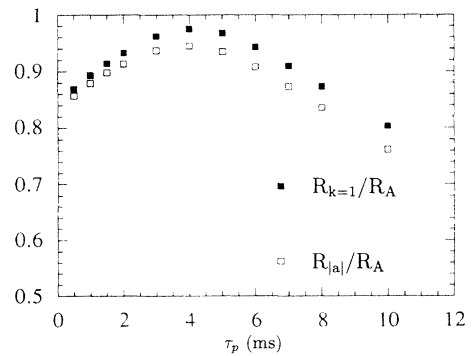


FIG. 3. Signal-to-noise ratio $R_{k=1}$ for the $k = 1$ component of the signal and that $R_{|a|}$ for the amplitude $|a|$, as a function of the pulse time constant τ_p . Both ratios are normalized to the signal-to-noise ratio R_A of a filter matched to the signal. To calculate $R_{|a|}$, $R_A = 4$. The signal is a pulse as in Eq. (30) with $\omega_p = \omega_1 = 2\pi \times 1$ kHz and $t_0 = 0$, while $q_{\text{opt}} = 30$ and $T = 20$ ms.

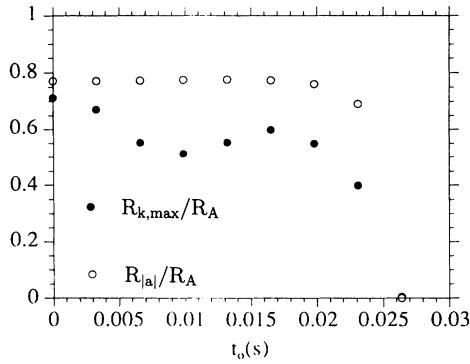


FIG. 4. Maximum signal-to-noise ratio $R_{k,\max}$ for one of the components of the signal and the signal-to-noise ratio $R_{|a|}$ on the amplitude $|a|$ as a function of the pulse delay t_0 . Both ratios are normalized to the signal-to-noise ratio R_A of a filter matched to the signal. To calculate $|a|$, $R_A = 4$. The signal is a pulse as in Eq. (30) with $\omega_p = \omega_1 = 2\pi \times 1$ kHz and $\tau_p = 0.5$ ms, while $q_{\text{opt}} = 30$ and $T = 50$ ms.

EXPERIMENTAL EXAMPLE

As an example of the experimental application of the method, we report here briefly some preliminary results obtained with a room temperature antenna [6]. A full discussion will appear elsewhere both for the practical algorithm developed [7] and for the experimental results [8].

The antenna is a 2.3-ton Al 5056 bar coupled to a capacitive resonant motion transducer [9] that converts the antenna displacement to an electric signal read by a field effect transistor (FET) amplifier. The total noise density at the FET output shows two lines, with frequencies $\nu_+ = 881.1$ Hz and $\nu_- = 863.6$ Hz, corresponding to the excitation of the two normal modes of the antenna-transducer system, merging into the wideband noise of the amplifier (Fig. 5).

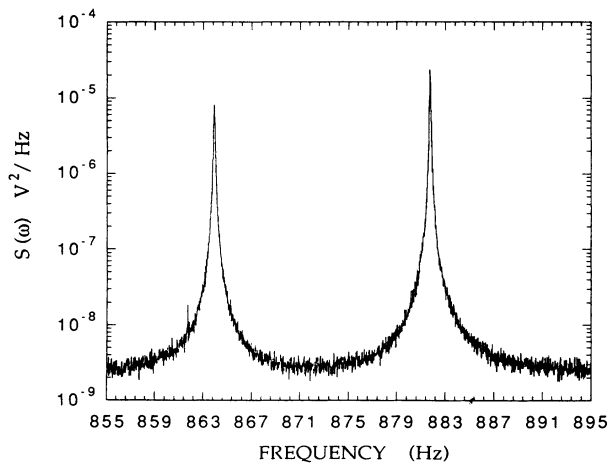


FIG. 5. Power spectrum $S(\omega)$ at the output of the room temperature antenna as a function of the frequency $\omega/2\pi$.

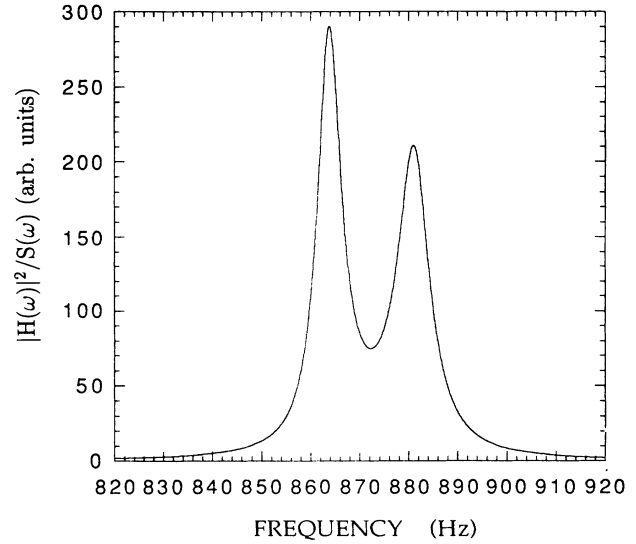


FIG. 6. Ratio of the transfer function square modulus $|H(\omega)|^2$ to the power spectrum $S(\omega)$ for the room temperature antenna, as a function of the frequency $\omega/2\pi$.

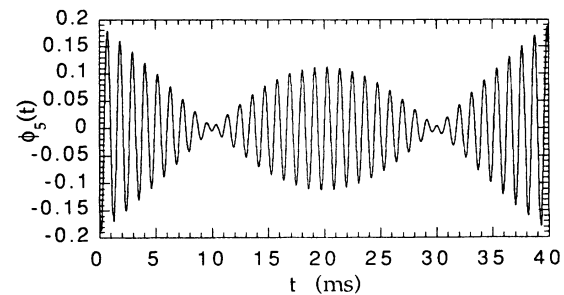
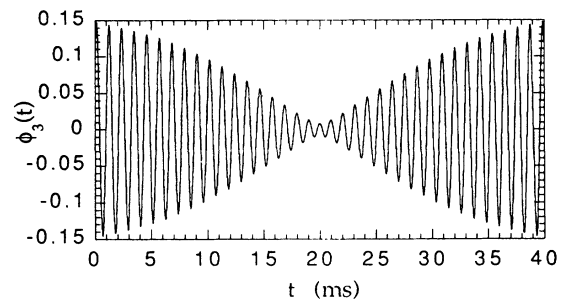
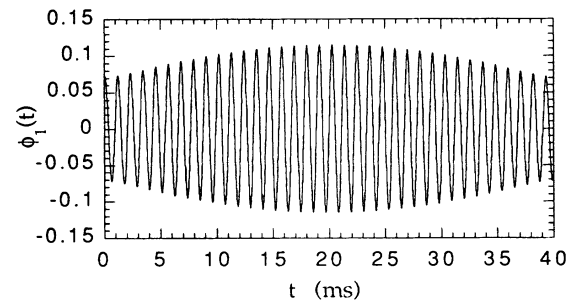


FIG. 7. First three even eigenfunctions $\phi_1(t)$, $\phi_3(t)$, and $\phi_5(t)$ for the room temperature, antenna, as a function of the time t .

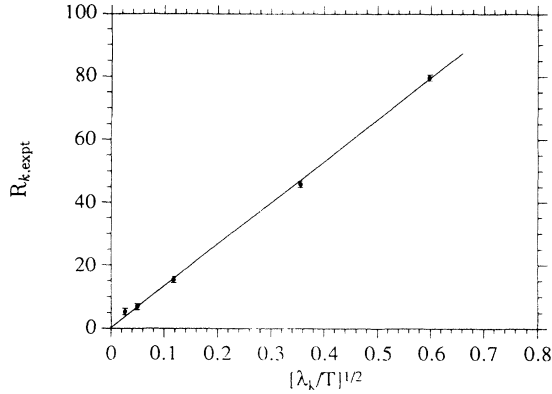


FIG. 8. Experimental signal-to-noise ratio $R_{k,\text{expt}}$ for the first four even eigenfunctions as a function of the ratio λ_k/T . λ_k is the calculated eigenvalue, and T is the duration of the measurement. Measurements have been made sending eigenfunctions of the same amplitude to the antenna input via a programmable function generator. The amplitude has been adjusted in order to have $R_{1,\text{expt}} \approx 80$.

In order to extract the transfer function $H(\omega)$, we have used a capacitive calibrator described in [10]. $H(\omega)$ is then the total transfer function for a voltage signal applied to the calibrator itself. $H(\omega)$ also includes all the filtering stages of the antenna electronics and of the data acquisition system.

Both the spectrum and transfer function show a two-peak structure and can be fitted to a ratio of polynomials. Their ratio can then be written as the factorizable function

$$\frac{|H(\omega)|^2}{S(\omega)} = \frac{\sum_{k=1}^4 \alpha_k (i\omega)^k}{\sum_{j=1}^4 \beta_j (i\omega)^j}. \quad (27)$$

As a consequence, the filter function $C_\delta(t)$ for the δ -like signal can be reduced to an Autoregressive moving average (ARMA) fourth-order filter [7,11]. The function $|H(\omega)|^2/S(\omega)$ is reported in Fig. 6. From the data in the figure, the two values of the post-detection bandwidths are of the order $1/2\pi\tau_{+\text{opt}} \approx 25$ Hz and $1/2\pi\tau_{-\text{opt}} \approx 19$ Hz.

The eigenfunctions of the integral equation (12) are then found numerically. In Fig. 7 the first few of them, corresponding to the largest eigenvalues, are shown for a choice of the maximum duration $T = 40$ ms. It can be seen that, despite the quite different shape of $C_\delta(\omega)$, the eigenfunctions retain the general form as in Eq. (24).

In order to test for the accuracy of the practical algorithm, we have applied to the calibrator voltage pulses shaped as the first few eigenfunctions of Eq. (12) and with variable amplitudes c_k . The pulses have been generated by a numerically programmable waveform generator. The output of the antenna has been sampled at 5 kHz, after a properly chosen antialiasing filter, for a time window of duration $T = 40$ ms starting after a suitable time lag from the beginning of the pulse. The data are then numerically filtered with the filter $C_\delta(\omega)$ and convoluted with the k th eigenfunction $\phi_k(t)$ to get the estimate of the relative amplitude \hat{c}_k .

In Fig. 8 we report the measured signal-to-noise ratio $R_{k,\text{expt}} = \hat{c}_k/\sigma_{k\text{ex}}$ as a function of the ratio λ_k/T . Here $\sigma_{k\text{ex}}$ is the rms fluctuation of the k th component *in the absence of the signal*. The amplitude of the input eigenfunctions were all equal and adjusted so that $R_{1,\text{expt}} = 80$.

DISCUSSION AND CONCLUSIONS

We have presented a novel application of the Karhunen-Loève expansion to the problem of measuring the statistically independent parameters of a gravitational wave pulse exciting a resonant antenna.

As the method has to be applied to a finite data window, one has to devise a way to partition the actual very long lasting flow of data, in segments of not too long a duration. In fact, as can be seen from the data in Fig. 2, if the duration T of the time window is much longer than the actual duration of the incoming signal, the signal-to-noise ratio both for the energy and for the amplitude of the first components starts to drop. On the other hand, the data in Fig. 4 show that if the time “center of mass” of the signal is displaced away from the center of the observation window, this does not affect very much the signal-to-noise ratio for the energy, provided that the signal still dies out within the observation window.

These considerations suggest a possible data reduction procedure as the one sketched in the following: The data have to be partitioned in windows of duration T . In order to maximize the signal-to-noise ratio, T has to be chosen of the order of the maximum duration of any expected signal. This points to a duration of the order of $T \approx 50$ ms [1]. The energy in each window is then evaluated as a test statistics to make a decision about the presence of a signal. In the case of an affirmative decision, the amplitudes of the components with significant signal-to-noise ratios are evaluated.

In order to avoid cutting off a signal too close to one of the edges of each time window, two neighboring windows should overlap by a substantial amount, a possible cautious choice for the overlap being one-half of the total duration of the window.

As an alternative, the time window could be shifted continuously and the energy in this running window of fixed duration T could be monitored. In the case of signal detection, the data within the window centered around the time at which the maximum energy has been detected could be further processed to extract the amplitudes of the various components.

Work is in progress to ascertain the practical feasibility and the possible refinements of the two methods above.

We conclude by noting that the method we have presented here can obviously be applied also to interferometric antennas, though in that case the basic features of the eigenfunctions would be rather different from those discussed here.

ACKNOWLEDGMENTS

It is a pleasure to acknowledge G. A. Prodi, L. Tafarello, and J. P. Zendri for letting us use the results

of the experiment with the room temperature antenna and M. Biasotto and G. Maron for helping us with the data acquisition system. It is also a great pleasure to acknowledge many deep and enlightening discussions with L. Tubaro.

APPENDIX

Many of the results of this appendix are well-known properties of integral equations or can be easily reduced to those. We report them here for the reader's convenience.

In order to evaluate the average value of E_T in Eq. (20) and its mean-square fluctuation, let us split the output $V'(t)$ of the δ -function filter into its noise part $n''(t)$ and its signal part $V_s''(t)$ with coefficients c_k as before:

$$\begin{aligned} V_s''(t) &= \int_{-\infty}^{\infty} dt' C_\delta(t-t') \int_0^{\infty} H(t'') h(t'-t'') dt'' \\ &= \int_{-\infty}^{\infty} G(t-t') h(t') dt' \\ &= \sum_{k=0}^{\infty} \lambda_k c_k \phi_k(t); \end{aligned} \quad (\text{A1})$$

then, the energy E_{sT} of $V''(t)$ in the interval $|t| \leq T/2$ is

$$E_{sT} = \int_{-T/2}^{T/2} (V_s'')^2(t) dt = \sum_{k=0}^{\infty} c_k^2 \lambda_k^2 = \sigma_\delta^2 \sum_{k=0}^{\infty} R_k^2 \lambda_k. \quad (\text{A2})$$

The mean value of E_T is then given by E_{sT} plus the noise contribution E_{nT} :

$$\langle E_{nT} \rangle = \sum_{k=0}^{\infty} \langle c_{nk}^2 \rangle \lambda_k^2 = \sigma_\delta^2 T, \quad (\text{A3})$$

where we have called c_{nk} the noise contribution to c_k . The variance of E_T is

$$\begin{aligned} \sigma_E^2 &= \left\langle \left[\sum_{k=1}^N \lambda_k^2 c_{nk}^2 + 2\lambda_k^2 c_k c_{nk} - \sigma_\delta^2 T \right]^2 \right\rangle \\ &= \sum_{k,j=1}^N \lambda_k^2 \lambda_j^2 [\langle c_{nk}^2 c_{nj}^2 \rangle + 4c_k c_j \langle c_{nk} c_{nj} \rangle] \\ &\quad + \sigma_\delta^4 T^2 - 2\sigma_\delta^2 T \sum_{k=1}^N \lambda_k^2 \langle c_{nk}^2 \rangle \\ &= 4\sigma_\delta^4 \left[\frac{1}{2} \sum_{k=1}^{\infty} \lambda_k^2 + \sum_{k=1}^{\infty} R_k^2 \lambda_k^2 \right], \end{aligned} \quad (\text{A4})$$

and the signal-to-noise ratio that we define by subtracting from $\langle E_T \rangle$ the mean noise contribution $\langle E_{nT} \rangle$ [Eq. (21)] follows.

The eigenfunction of Eq. (12) with $G(t)$ given by Eq. (22) has to solve the differential equation

$$\frac{d^2 \phi_k}{dt^2} + \left(2\omega_1^2 - \frac{1}{\tau_{\text{opt}}^2} \right) \frac{d\phi_k}{dt} + \omega_0^4 \left(1 - \frac{2}{\lambda_k \omega_1^2 \tau_{\text{opt}}} \right) \phi_k = 0, \quad (\text{A5})$$

with the boundary conditions

$$\left(\frac{d^2 \phi_k}{dt^2} \right)_{t=-T/2} - \frac{1}{\tau_{\text{opt}}} \left(\frac{d\phi_k}{dt} \right)_{t=-T/2} + \omega_1^2 \phi_k(-T/2) = 0, \quad (\text{A6a})$$

$$\left(\frac{d^3 \phi_k}{dt^3} \right)_{t=-T/2} - \frac{1}{\tau_{\text{opt}}} \left(\frac{d^2 \phi_k}{dt^2} \right)_{t=-T/2} + \omega_1^2 \left(\frac{d\phi_k}{dt} \right)_{t=-T/2} = 0,$$

$$\left(\frac{d^2 \phi_k}{dt^2} \right)_{t=T/2} + \frac{1}{\tau_{\text{opt}}} \left(\frac{d\phi_k}{dt} \right)_{t=T/2} + \omega_1^2 \phi_k(T/2) = 0, \quad (\text{A6b})$$

$$\left(\frac{d^3 \phi_k}{dt^3} \right)_{t=T/2} + \frac{1}{\tau_{\text{opt}}} \left(\frac{d^2 \phi_k}{dt^2} \right)_{t=T/2} + \omega_1^2 \left(\frac{d\phi_k}{dt} \right)_{t=T/2} = 0.$$

As $G(t)$ is an even function, for nondegenerate eigenvalues λ_k the eigenfunctions have to be either even or odd. As a consequence, they have to be of one of the two forms in Eq. (24). The eigenvalues can be found by substituting Eq. (24), for instance, in Eqs. (A6a) and by asking that the determinant of the resulting homogeneous system for A_{k+} and A_{k-} be equal to zero.

- [1] See, for instance, D. Blair, *The Detection of Gravitational Waves* (Cambridge University Press, Cambridge, England, 1991), Chap. 2.
- [2] M. Cerdonio, A. Ortolan, G. A. Prodi, S. Vitale, and J. P. Zendri, in *TAUP 93*, Proceedings of the Third International Workshop on Theoretical and Phenomenological Aspects of Underground Physics, Gran Sasso, Italy, edited by C. Arpesella *et al.* [Nucl. Phys. B (Proc. Suppl.) **35**, 75 (1994)].
- [3] See, for instance, C. W. Helstrom, *Statistical Theory of Signal Detection* (Pergamon, Oxford, 1968), Chap. IV.
- [4] R. Giffard, Phys. Rev. D **14**, 2478 (1976).
- [5] E. Amaldi and G. Pizzella, in *Relativity Quanta and Cos-*

mology, edited by F. De Finis (Johnson, New York, 1979), p. 5.

- [6] M. Cerdonio *et al.*, in *Proceedings of the 10th Italian Conference on General Relativity and Gravitational Physics*, Bardonecchia, Italy (World Scientific, Singapore, in press).
- [7] G. Vedovato *et al.* (in preparation).
- [8] G. A. Prodi *et al.* (in preparation).
- [9] Y. Ogawa and P. Rapagnani, Nuovo Cimento C **7**, 21 (1984).
- [10] S. Paoli, thesis, University of Trento, 1993.
- [11] A. Papoulis, *Probability, Random Variables, and Stochastic Processes* (McGraw-Hill, Singapore, 1984).